EUROPEAN JOURNAL OF PURE AND APPLIED MATHEMATICS
Vol. 2, No. 3, 2009, (401-425)
ISSN 1307-5543 – www.ejpam.com

Flocking of Multi-agents in Constrained Environments

Bibhya Sharma*, Jito Vanualailai and Utesh Chand

School of Computing, Information & Mathematical Sciences, University of the South Pacific, Suva, FIJI

Abstract. Flocking, arguably one of the most fascinating concepts in nature, has in recent times established a growing stature within the field of robotics. In this paper, we control the collective motion of a flock of nonholonomic car-like vehicles in a constrained environment. A continuous centralized motion planner is proposed for split/rejoin maneuvers of the flock via the Lyapunov-based control scheme to anchor avoidance of obstacles intersecting the paths of flockmates. The control scheme inherently utilizes the artificial potential fields, within a new leader-follower framework, to accomplish the desired formations and reformations of the flock. The effectiveness of the proposed control laws are demonstrated through computer simulations.

2000 Mathematics Subject Classifications: 34A30, 34D20, 70E60, 93C85, 93D15.

Key Words and Phrases: Multi-agents, Lyapunov-based control scheme, split/rejoin, cooperating, flocking.

*Corresponding author.

Email address: sharma_b@usp.ac.fj (B. Sharma)

1. Introduction

Flocking is a coordinate and cooperative behavior easily conspicuous in a large number of beings, ranging from simple bacteria to mammals [8]. Prominent examples from nature include: schools of fishes, flocks of birds, and herds of animals, to name a few. This salient behavior is predominantly based on the principle that there is safety and strength in numbers [4, 5]. For example, a flock of birds invariably demonstrates a larger entity and dissuades potential attackers. On the other hand, if a flock is attacked the flockmates can scatter to confuse the predators, thus avoid being captured, then regroup at a safer distance. Flocking behavior also contributes to cooperative foraging, better opportunities for mating and safer long distance migrations [6]. Flocks travelling in large dense groups are capable of smooth collision and obstacle avoidance maneuvers even in the presence of external obstacles which may be fixed or even moving.

In literature, the flocking models are built within a framework of three basic rules of steering namely, separation, alignment, and cohesion, which describe how an individual maneuvers based on the positions and velocities of its nearby flockmates [12]. Although the rules governing each member of a flock are seemingly basic, the collective motion is strikingly spectacular. The superposition of these rules results in the flockmates moving in a particular formation, with a common heading whilst ensuring all possible collision and obstacle avoidances [16].

Biologically inspired algorithms that mimic the flocking behavior are essential in accomplishing the control objective of a group while also ensuring a collision-free flightpath. Common objectives nowadays include formation flight control, satellite clustering, exploration, surveillance, foraging and cooperative manipulation [1, 3, 8]. The applications of foraging could involve search-and-rescue teams at disaster sites. Team(s) of robots can be deployed to collect hazardous materials after a spill or other

accidents in minimal time, hence, saving further loss. All in all, team(s) of homogenous (even heterogenous) robots working towards a common objective can satisfy stringent time, manpower and monetary demands, enhance performances and robustness, and harness desired multi-behaviors, each of which is extremely difficult if not entirely impossible to obtain from single agents [5, 7, 9, 11].

A wide spectrum of approaches have appeared in literature in relation to "formation stiffness", a rule necessitating strict observance of the prescribed formation during the motion of the flock [13, 15]. On one end we have the *split/rejoin* maneuvers. The applicability of the split/rejoin maneuvers can be immediately obvious in the field of robotics, for example, reconnaissance, sampling, and surveillance. Populating the other end of the spectrum are the *tight-formations* which can be required in applications that require cooperative payload transportation [3, 9, 13, 15]. The main strength of this paper lies on the emphasis placed upon the split/rejoin maneuvers, where a group of robots in a specific formation splits and moves around the encountering obstacle(s) and then returns to take its original position in the prescribed formation. A new strategy is introduced in this paper to induce the split/rejoin maneuvers.

In recent times robotic applications with split/rejoin maneuvers have become increasingly popular [3, 17, 18]. We will mention a few important ones here. Chang *et al.* [3] used gyroscopic forces and scalar potential techniques to create swarming behaviors for multiple agent systems. The governing decentralized control law guaranteed a group of robots accomplish specified control objectives while avoiding inter-robot collisions and with unforeseen obstacles. [17, 18] provided design and analysis of distributed algorithms for large number of dynamic agents that enabled the group to perform coordinated tasks. Free-flocking and flocking with obstacle avoidance were considered with split/rejoin and squeezing maneuvers. Recently Sharma *et al.* [14, 15] and Vanualailai *et al.* [19] developed algorithms that considered motion planning and control of mobile robots within a constrained and obstacle-ridden

workspace. Continuous acceleration-based control laws derived from the Lyapunov-based control scheme were utilized in their studies. In brief, the Lyapunov-based control scheme is a new artificial potential field method which basically involves attaching attractive fields to the target and repulsive fields to each of the obstacles [10]. The total potential of the workspace is the sum of the attractive and repulsive fields generated within the framework of the control scheme. The reader is referred to [13] for a detailed account of the control scheme. Inspired, we adopt the control scheme to control the flocking motion of a group of nonholonomic car-like vehicles. This paper will demonstrate how the group can avoid collision with fixed obstacles by scattering, and then regrouping after executing a successful avoidance maneuver. This avoidance maneuver will be the split/rejoin maneuver, the coin of realm of the research. In parallel, the control scheme utilizes Lyapunov's Direct Method to analyze stability of the vehicular system.

This paper is organized as follows: in Section 2 the robot model is defined; in Section 3 motion planning is carried out, defining the targets, obstacles, and appropriate attractive and avoidance functions; in Section 4 the Lyapunov-based control scheme is executed to yield the controllers and to analyze the stability of the robot system; in Section 5 we illustrate the effectiveness of the proposed controllers via simulations involving the required split/rejoin maneuvers; and in Section 6 we conclude the paper and outline future work in the area.

2. Boid Model

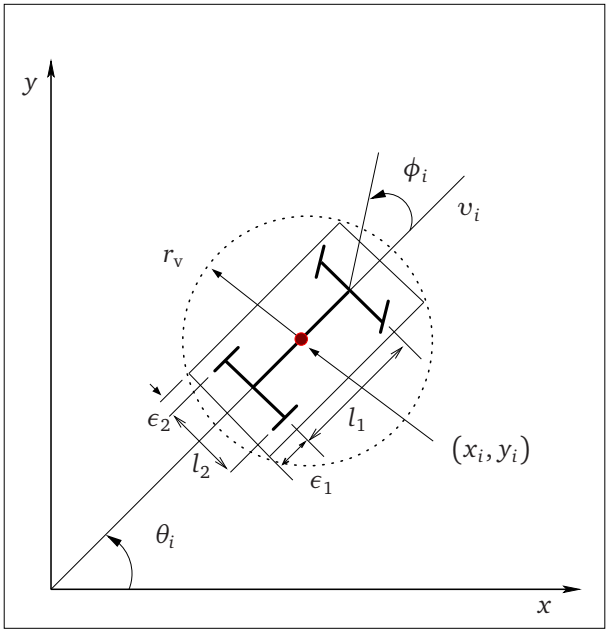

Figure 1: Kinematic model of ith boid.

Following the nomenclature of Reynolds [12], we denote each member of the flock as a *boid*. In addition, each boid is assumed to be a front-wheel steered car-like vehicle, whereby engine power is applied to the rear wheels.

With reference to Fig. 1, (x_i, y_i) denotes the CoM of the ith boid, θ_i gives its angle with respect to the x-axis of the main frame, ϕ_i gives the steering wheel's angle with respect to the ith boid's longitudinal axis. For simplicity, the dimensions of the n boids are kept the same. Therefore, l_1 is the distance between the center of the rear and front axles, while l_2 is the length of each axle.

The configuration of the ith boid is given by $(x_i, y_i, \theta_i, \phi_i) \in \mathbb{R}^4$, and its position is given as the point $(x_i, y_i) \in \mathbb{R}^2$. The kinodynamic model of the ith boid, adopted from [14], with respect to its CoM is

$$\left.\begin{aligned} \dot{x}_i &= \upsilon_i \cos\theta_i - \tfrac{l_1}{2}\omega_i \sin\theta_i \ , \\ \dot{y}_i &= \upsilon_i \sin\theta_i + \tfrac{l_1}{2}\omega_i \cos\theta_i \ , \\ \dot{\theta}_i &= \omega_i \ , \quad \dot{\upsilon}_i = \sigma_i \ , \\ \dot{\omega}_i &= \eta_i \ , \quad \text{for } i = 1, \ldots, n, \end{aligned}\right\} \tag{2.1}$$

where υ_i and ω_i are, respectively, the instantaneous translational and rotational velocities, while σ_i and η_i are the instantaneous translational and rotational accelerations of the ith boid. Without any loss of generality, we assume $\phi_i = \theta_i$. The state of ith boid is captured by the vector notation $\boldsymbol{x}_i := (x_i, y_i, \theta_i, \upsilon_i, \omega_i) \in \mathbb{R}^5$, $i = 1, 2, ..., n$. For n boids, we define the vector $\boldsymbol{x} = (\boldsymbol{x}_1, ..., \boldsymbol{x}_n) \in \mathbb{R}^{5\times n}$. Given the *clearance parameters* ϵ_1 and ϵ_2, we can enclose each boid by a protective circular region (smallest possible) centered at (x_i, y_i), with radius $r_{\text{v}} = \sqrt{(l_1 + 2\epsilon_1)^2 + (l_2 + 2\epsilon_2)^2}/2$. The representation not only maximizes the free space available to the robots in the workspace but it also ensures an easier construction of the potential field functions ([13], [14]).

3. Devising the problem

In this section we formulate the split/rejoin maneuver for a flock of n nonholonomic boids, guided by a leader-follower strategy. In a split/rejoin maneuver a flock maintained in a prescribed formation splits and moves around encountering obstacle(s) and then returns to take its original position in the original formation.

The Lyapunov-based control scheme requires the design of *target attractive functions* and *obstacle avoidance functions*. On one hand, a attractive potential field function will be constructed from each target attractive function. This will enable a boid to move towards its designated targets whilst maintaining the overall formation. On the other hand, a repulsive potential field function would be designed from each obstacle avoidance function constructed. This will ensure a collision-free avoidance in the workspace. Next, these artificial potential field functions would be integrated ap-

propriately to form a Lyapunov function (total potentials) from which the controllers would be generated.

3.1. Attractive Potential Field Functions

To formulate functions that instigate attraction of the boids towards their designated targets we, first and foremost, need to introduce a new leader-follower strategy. This new strategy helps in establishing and maintaining prescribed formations.

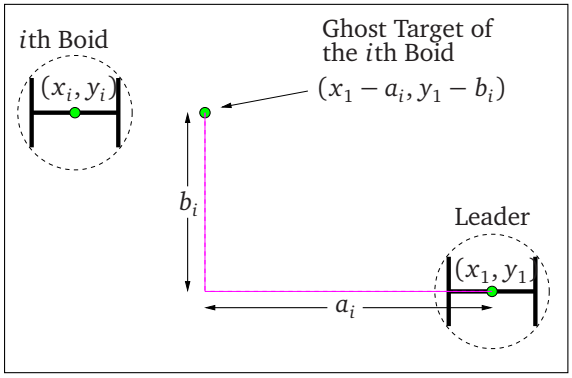

Figure 2: Positioning of a mobile ghost target relative to the position of the leader-boid.

The new leader-follower strategy summons the boids of the flock to follow one particular boid which is adopted as the leader-boid. This strategy is advocated for the very first time via *mobile ghost targets*. These ghost targets are positioned relative to the position of the leader-boid with a user defined Euclidean measure (Figure 2).

We note here that each follower-robot will have a different mobile ghost target designated to it.

While the mobile ghost targets move relative to the position of the leader-boid, the follower-boids move towards the ghost targets designated to them, at every iteration $t > 0$.

3.1.1. Attraction to Target/Ghost Target

For the ith boid, we designate a target

$$T_i = \{(x, y) \in \mathbb{R}^2 : (x - t_{i1})^2 + (y - t_{i2})^2 \leq r t_i^2\}$$

with center (t_{i1}, t_{i2}) and radius $r t_i$. The leader-boid (i=1) will move towards its target with center (t_{11}, t_{12}). Now, with respect to the follower-boids, the mobile ghost targets allocated to each will be positioned relative to the position of the leader (a_i horizontal units and b_i vertical units, see Fig. 2) and whose center is given by $(t_{i1}, t_{i2}) = (x_1 - a_i, y_1 - b_i)$, for $i = 2$ to n.

For attraction to the target/ghost target, we shall use an attractive function of the form

$$H_{N_i}(\boldsymbol{x}) = \frac{1}{2} \ln(H_i + 1)\,,$$

where

$$H_i(\boldsymbol{x}) = (x_i - t_{i1})^2 + (y_i - t_{i2})^2 + \upsilon_i^2 + \omega_i^2\,, \text{ for } i = 1, \ldots, n. \tag{3.1}$$

While the function is the measure of the distance between the ith boid and its target T_i, it can also be treated as a measure of its convergence. In this case, the particular form of $H_{N_i}(\boldsymbol{x})$ is sufficient to be treated as a suitable attractive potential function required to generate attractive fields around the targets. Figure 3(a) shows the valleys created by the attractive forces in a continuous potential field. These mobile valleys, associated to the mobile ghost targets of the follower-boids 1 and 2, are positioned according to user-defined measurements in the leader-follower scheme. Similarly, there would be a valley each for the remaining flockmates and the ultimate goal is for each follower-boid to move to its designated valley. Figure 3(b) shows the accompanying contour plot.

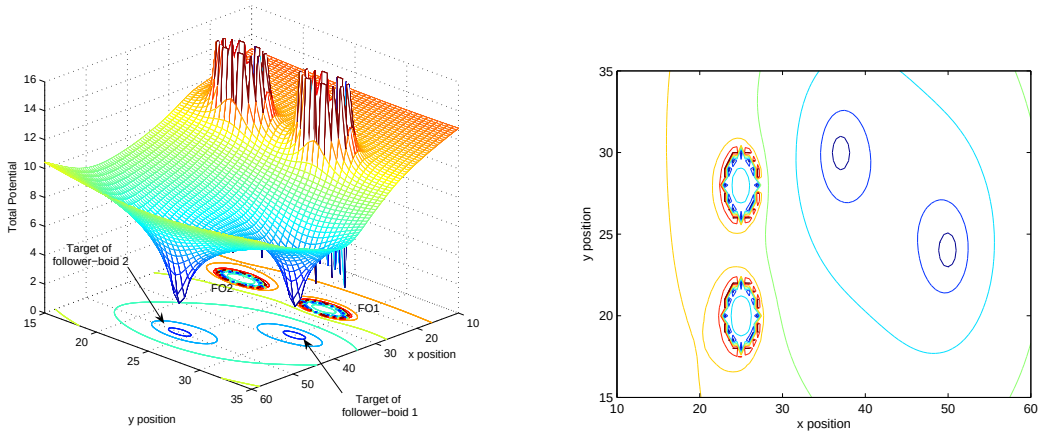

(a) 3D visualization (b) Contour Plot

Figure 3: Total potential and the contour plot generated using the attractive potential function for target attraction and the repulsive potential function for avoidance of disk-shaped obstacles.

3.1.2. Auxiliary Function

To ensure that the Lyapunov function candidate vanishes when all the boids converge to their final target configuration we design a new attractive function whose role is purely mathematical, and hence, auxiliary. We define this auxiliary function as

$$G_i(\boldsymbol{x}) = \frac{1}{2}\left[(x_i - t_{i1})^2 + (y_i - t_{i2})^2 + (\theta_i - t_{i3})^2\right] \geq 0\,, \quad \text{for } i = 1, \ldots, n, \tag{3.2}$$

where t_{i3} is the desired orientation of the ith boid. We will multiply the function to each of the repulsive potential field function to be designed in the following section.

3.2. Repulsive Potential Field Functions

We desire the boids to avoid all fixed and moving obstacles intersecting their paths. Therefore, we construct obstacle avoidance functions that basically measure the distances between the ith boid and obstacles in the workspace. To obtain the desired

avoidance, each of these functions will appear in the denominator of the repulsive potential field function to generate the repulsive fields around the obstacles. The numerators will be populated by *tuning parameters* which may be refined for safer, shorter and smoother trajectories. The reader is referred to [13, 14, 19] for further explanations. Now, we describe each obstacle appearing in the constrained workspace and design the associated avoidance function.

3.2.1. Stationary Obstacles

Let $O_q, q \in \{1, \ldots, m\}$, represent a solid object fixed within the workspace. We provide the following definition of the stationary obstacles

Definition 3.1. *The kth stationary obstacle is a disk with center* (o_{k1}, o_{k2}) *and radius* ro_k. *Precisely, the kth stationary obstacle fixed in the workspace is the set*

$$O_k = \{(z_1, z_2) \in \mathbb{R}^2 : (z_1 - o_{k1})^2 + (z_2 - o_{k2})^2 \leq ro_k\}.$$

For the ith boid to avoid the kth stationary obstacle, we adopt the avoidance function

$$W_{ik}(\boldsymbol{x}) = \frac{1}{2}\left[(x_i - o_{k1})^2 + (y_i - o_{k2})^2 - \left(ro_k + r_{\text{v}}\right)^2\right], \text{ for } i = 1, \ldots, n \ ; \ k = 1, \ldots, m. \tag{3.3}$$

This positive function is the Euclidean measure of the distance between the ith boid and the kth stationary obstacle. Now let us consider, for some constant $\alpha_{ik} > 0$ (classified as a tuning parameter), for $i = 1$ (leader-boid) and $k = 1$ (a stationary obstacle fixed in the workspace), the effect of the ratio $\frac{\alpha_{11}}{W_{11}}$. According to the Lyapunov-based control scheme, this ratio is classified as a *repulsive potential field function*. If the leader-boid approaches the stationary obstacle, then the value of the ratio will increase. If it moves away from the stationary obstacle, the ratio will decrease.

Now, to provide the importance of the Lyapunov-based control scheme, we assume that the ratio is an appropriate part of a Lyapunov function, L, which forms the

artificial potential field function for system (2.1). Because, with respect to time $t \geq 0$, one gets $dL/dt \leq 0$ along a trajectory of (2.1), and L is a positive definite function, L cannot increase in t. Therefore any change in the value of the ratio could only correspond to either an increase or decrease in $|dL/dt|$. Analogously, $|dL/dt|$ is the rate of dissipation of energy from the system in absolute value. If the stationary solid object is being approached, then W_{11} gets smaller, and the ratio gets larger. Thus, the rate of energy dissipation, in absolute value, gets larger. This, in turn, results in an increased activity of the system. This increased activity could only be directed towards a stable equilibrium point, away from the stationary solid object. In other words, a situation where $W_{11} = 0$ can never eventuate. Hence, if the ratio is a part of a Lyapunov function for system (2.1), then intuitively the ratio will act as a *repulsive potential field function*, this is the very essence of the Lyapunov-based control scheme. An example of the effect of the repulsive potential function designed from Equation (3.3) can be seen in Figure 3(a). The cylindrical potential spikes are immediately evident.

Henceforth, all the obstacle avoidance functions will be appropriately coupled with tuning parameters to design the repulsive potential field functions to generate the collision and obstacle avoidance maneuvers.

3.2.2. Moving Obstacles

From a practical viewpoint, the control algorithms must generate feasible trajectories based upon real-time perceptual information. In this paper, we will only consider moving obstacles of which the system has complete and *a priori* knowledge. Here, each boid itself becomes a moving obstacle for all the other boids. Therefore, for the ith boid to avoid the jth moving boid, we consider

$$V_{ij}(\boldsymbol{x}) = \frac{1}{2}\left[(x_i - x_j)^2 + (y_i - y_j)^2 - \left(2 \times r_{\mathrm{v}}\right)^2\right], \quad \text{for } i, j = 1 \ldots, n,\ i \neq j. \tag{3.4}$$

This avoidance function is the measure of the Euclidean distance between the ith and the jth boid.

3.2.3. Dynamics Constraints

Again, in practice, the translational speed and the steering angle of the robots are limited. However, in order to treat the dynamic constraints within the Lyapunov-based control scheme we will have design an *artificial obstacle* corresponding to each dynamic constraint. Following on, we will design an appropriate obstacle avoidance function for its avoidance.

If $v_{max} > 0$ is the maximum speed, and ϕ_{max} is the maximum steering angle satisfying $0 < \phi_{max} < \frac{\pi}{2}$ then, as shown in [14], the constraints imposed on the translational and the rotational velocities are $|v_i| < v_{max}$ and $v_i^2 \geq \rho_{min}^2 \omega_i^2$. Where ρ_{min} known as the *minimum turning radius* is given as $\rho_{min} = \frac{l_1}{\tan \phi_{max}}$. From above we get $|\omega_i| \leq \frac{|v_i|}{|\rho_{min}|} < \frac{v_{max}}{|\rho_{min}|}$.

Based on these constraints, the following artificial obstacles can be constructed:

$$AO_{i1} = \{v_i \in \mathbb{R} : v_i \leq -v_{\max} \text{ or } v_i \geq v_{\max}\},$$
$$AO_{i2} = \{\omega_i \in \mathbb{R} : \omega_i \leq -v_{\max}/|\rho_{\min}| \text{ or } \omega_i \geq v_{\max}/|\rho_{\min}|\},$$

For avoidance, the following obstacle avoidance functions will be included:

$$U_{i1}(\boldsymbol{x}) = \frac{1}{2}(v_{max} - v_i)(v_{max} + v_i)\,, \tag{3.5}$$
$$U_{i2}(\boldsymbol{x}) = \frac{1}{2}\left(\frac{v_{max}}{|\rho_{min}|} - \omega_i\right)\left(\frac{v_{max}}{|\rho_{min}|} + \omega_i\right), \quad \text{for } i = 1, \ldots, n. \tag{3.6}$$

The repulsive potential functions generated from these obstacle avoidance functions would guarantee the adherence to the limitations placed upon translational velocity v_i and the steering angle ϕ_i, respectively.

4. Lyapunov-based Control Scheme

Utilizing the Lyapunov-based control scheme we now design the nonlinear control laws and provide a mathematical proof that system (2.1) is indeed stable. The control laws have been extracted from a Lyapunov function which appropriately sums the attractive and repulsive potential field functions designed in the aforementioned sections.

We begin with the following theorem:

Theorem 4.1. *Consider a flock of nonholonomic boids, the motion of which is governed by ODEs described by system (2.1). The objective is to, amongst considering other integrated subtasks, establish and control a prescribed formation, facilitate split/rejoin maneuvers of the boids within a constrained environment and reach the target configuration with the original formation. The subtasks include; restrictions placed on the workspace, convergence to predefined targets, and consideration of kinematic and dynamic constraints. Utilizing the attractive and repulsive potential field functions the following continuous time-invariant control laws can be generated for the ith boid that* per se *stabilizes system (2.1) as well:*

$$\sigma_i = -\left[\delta_{i1}\upsilon_i + f_{1i}\cos\theta_i + f_{2i}\sin\theta_i\right]/f_{4i}\,, \tag{4.1}$$

$$\eta_i = -\left[\delta_{i2}\omega_i + \frac{l_l}{2}\left(-f_{1i}\sin\theta_i + f_{2i}\cos\theta_i\right) + f_{3i}\right]/f_{5i}\,, \tag{4.2}$$

for $i = 1$ to n where $\delta_{i1}, \delta_{i2} > 0$ are constants commonly known as convergence parameters.

Proof:

Introducing positive constants, denoted as *tuning parameters*, $\alpha_{ik} > 0$, $\beta_{ij} > 0$ and $\gamma_{is} > 0$, for $i, j, k, s \in N$, we propose a Lyapunov function candidate for system (2.1):

$$L(\boldsymbol{x}) = \sum_{i=1}^{n}\left\{H_{N_i}(\boldsymbol{x}) + G_i(\boldsymbol{x})\left[\sum_{k=1}^{m}\frac{\alpha_{ik}}{W_{ik}(\boldsymbol{x})} + \sum_{s=1}^{2}\frac{\gamma_{is}}{U_{is}(\boldsymbol{x})} + \sum_{j=1,i\neq j}^{n}\frac{\beta_{ij}}{V_{ij}(\boldsymbol{x})}\right]\right\}. \tag{4.3}$$

Assumption 4.1. $\boldsymbol{x}^* = (t_{i1}, t_{i2}, t_{i3}, 0, 0, \ldots, t_{n1}, t_{n2}, t_{n3}, 0, 0) \in \mathbb{R}^{5n} \in D(L)$ *is an equilibrium point of system (2.1).*

Remark 4.1. *This is a reasonable assumption since* $\dot{L}(\boldsymbol{x}^*) = 0$ *making* $\boldsymbol{x}^*$ *a feasible equilibrium point, at least, in a small neighborhood of the target configuration.*

Then one can easily verify the following:

1. L is continuous and positive on the domain $\mathbb{D}$ given as

$$\begin{aligned} D(L) \;=\; \{\, \boldsymbol{x} \in \mathbb{R}^{5\times n} :\; & W_{ik}(\boldsymbol{x}) > 0 \text{ for } i = 1 \text{ to } n\,,\; k = 1 \text{ to } m\,,\; U_{is}(\boldsymbol{x}) > 0 \text{ for} \\ & i = 1 \text{ to } n\,,\; s = 1 \text{ to } 2 \;\text{ and }\; V_{ij}(\boldsymbol{x}) > 0 \text{ for } i, j = 1 \text{ to } n\,,\; i \neq j \,\}\,. \end{aligned}$$

2. $L(\boldsymbol{x}^*) = 0,\ \boldsymbol{x}^* \in \mathbb{D}$.

3. $L(\boldsymbol{x}) > 0 \;\; \forall\, \boldsymbol{x} \in \mathbb{D}, \boldsymbol{x} \neq \boldsymbol{x}^*$.

Now let us consider the time derivative of our Lyapunov function candidate $L(\boldsymbol{x})$. Along a particular trajectory of system (2.1), we have, upon collecting terms with v_i and ω_i separately

$$\begin{aligned} \dot{L}_{(2.1)}(\boldsymbol{x}) \;=\; & \sum_{j=1}^{n} \Big[\, \left(f_{1i}\cos\theta_i + f_{2i}\sin\theta_i + f_{4i}\sigma_i\right) v_i \\ & -\; \left(\frac{l_1}{2} f_{1i}\sin\theta_i - \frac{l_1}{2} f_{2i}\cos\theta_i - f_{3i} - f_{5i}\eta_i\right) \omega_i \Big]\,, \end{aligned}$$

where functions f_{1i} to f_{5i} are defined as (on suppressing $\boldsymbol{x}$):

$$\begin{aligned} f_{11} \;=\; & \left(\frac{1}{H_1+1} + \sum_{k=1}^{m}\frac{\alpha_{1k}}{W_{1k}} + \sum_{s=1}^{2}\frac{\gamma_{1s}}{U_{1s}} + \sum_{j=2}^{n}\frac{\beta_{1j}}{V_{1j}}\right)(x_1 - t_{11}) \\ & -\sum_{i=2}^{n}\left(\frac{1}{H_i+1} + \sum_{k=1}^{m}\frac{\alpha_{ik}}{W_{ik}} + \sum_{s=1}^{2}\frac{\gamma_{is}}{U_{is}} + \sum_{j=1, i\neq j}^{n}\frac{\beta_{ij}}{V_{ij}}\right)(x_i - t_{i1}) \\ & -G_1\sum_{j=2}^{n}\frac{\beta_{1j}}{V_{1j}^2}(x_1 - x_j) + \sum_{j=2}^{n} G_j\frac{\beta_{j1}}{V_{j1}^2}(x_j - x_1) - G_1\sum_{k=1}^{m}\frac{\alpha_{1k}}{W_{1k}^2}(x_1 - o_{k1})\,, \end{aligned}$$

$$
\begin{aligned}
f_{1i} &= \left(\frac{1}{H_i+1}+\sum_{k=1}^{m}\frac{\alpha_{ik}}{W_{ik}}+\sum_{s=1}^{2}\frac{\gamma_{is}}{U_{is}}+\sum_{j=1,i\neq j}^{n}\frac{\beta_{ij}}{V_{ij}}\right)(x_i-t_{i1})\\
&\quad -G_i\sum_{j=1,i\neq j}^{n}\frac{\beta_{ij}}{V_{ij}^2}(x_i-x_j)+\sum_{j=1,i\neq j}^{n}G_j\frac{\beta_{ji}}{V_{ji}^2}(x_j-x_i)-G_i\sum_{k=1}^{m}\frac{\alpha_{ik}}{W_{ik}^2}(x_i-o_{k1}),
\end{aligned}
$$

for $i=2$ to n ,

$$
\begin{aligned}
f_{21} &= \left(\frac{1}{H_1+1}+\sum_{k=1}^{m}\frac{\alpha_{1k}}{W_{1k}}+\sum_{s=1}^{2}\frac{\gamma_{1s}}{U_{1s}}+\sum_{j=2}^{n}\frac{\beta_{1j}}{V_{1j}}\right)(y_1-t_{12})\\
&\quad -\sum_{i=2}^{n}\left(\frac{1}{H_i+1}+\sum_{k=1}^{m}\frac{\alpha_{ik}}{W_{ik}}+\sum_{s=1}^{2}\frac{\gamma_{is}}{U_{is}}+\sum_{j=1,i\neq j}^{n}\frac{\beta_{ij}}{V_{ij}}\right)(y_i-t_{i2})\\
&\quad -G_1\sum_{j=2}^{n}\frac{\beta_{1j}}{V_{1j}^2}(y_1-y_j)+\sum_{j=2}^{n}G_j\frac{\beta_{j1}}{V_{j1}^2}(y_j-y_1)-G_1\sum_{k=1}^{m}\frac{\alpha_{1k}}{W_{1k}^2}(y_1-o_{k2}),
\end{aligned}
$$

$$
\begin{aligned}
f_{2i} &= \left(\frac{1}{H_i+1}+\sum_{k=1}^{m}\frac{\alpha_{ik}}{W_{ik}}+\sum_{s=1}^{2}\frac{\gamma_{is}}{U_{is}}+\sum_{j=1,i\neq j}^{n}\frac{\beta_{ij}}{V_{ij}}\right)(y_i-t_{i2})\\
&\quad -G_i\sum_{j=1,i\neq j}^{n}\frac{\beta_{ij}}{V_{ij}^2}(y_i-y_j)+\sum_{j=1,i\neq j}^{n}G_j\frac{\beta_{ji}}{V_{ji}^2}(y_j-y_i)-G_i\sum_{k=1}^{m}\frac{\alpha_{ik}}{W_{ik}^2}(y_i-o_{k2}),
\end{aligned}
$$

for $i=2$ to n , and

$$
f_{3i} = \left(\sum_{k=1}^{m}\frac{\alpha_{ik}}{W_{ik}}+\sum_{s=1}^{2}\frac{\gamma_{is}}{U_{is}}+\sum_{j=1,i\neq j}^{n}\frac{\beta_{ij}}{V_{ij}}\right)(\theta_i-t_{i3}),
$$

$$
f_{4i} = \frac{1}{H_i+1}+G_i\frac{\gamma_{i1}}{U_{i1}^2},\ f_{5i}=\frac{1}{H_i+1}+G_i\frac{\gamma_{i2}}{U_{i2}^2},
$$

for $i=1$ to n.

Substituting the controllers given in (4.1) - (4.2) and the governing ODEs for system (2.1) we obtain a semi-negative definite function :

$$
\dot{L}_{(2.1)}(\boldsymbol{x})=-\sum_{i=1}^{n}\left(\delta_{i1}v_i^2+\delta_{i2}\omega_i^2\right)\leq 0\,.
$$

We have thus provided a working proof of the fact that $\frac{d}{dt}[L(\boldsymbol{x})] \leq 0 \ \ \forall \ \boldsymbol{x} \in \mathbb{D}$.

Finally, it can easily be verified that the first partials of $L_{(2.1)}(\boldsymbol{x})$ is C^1 which makes up the fifth and final prerequisite of a Lyapunov function.

Once $L(\boldsymbol{x})$ successfully meets the five prerequisites discussed above, it is declared a feasible Lyapunov function for system (2.1) and $\boldsymbol{x}^*$ is at least a stable equilibrium point in the sense of Lyapunov. In our case, this practical limitation is well within the Lyapunov framework and there is no contradiction with Brockett's result [2] because we have proven only stability, and not asymptotic stability. Stability means that any solution of system (2.1) starting close to $\boldsymbol{x}^*$ remains near it at all times.

5. Results

In this section we illustrate the effectiveness of the Lyapunov-based control scheme and the resulting nonlinear control laws, by simulating two interesting scenarios. We present two different split/rejoin maneuvers for a flock of ten boids clustered at the starting line. The boids in each scenario coalesce into a distinct prescribed formation and move in the direction of their targets. When the formation encounters fixed obstacles intersecting its path, the affected boids split and move around the obstacles for a collision-free avoidance. Subsequently, the boids rejoin their coherent group and the original formation gets re-enacted before the final target position is attained.

We consider two different formations in this paper: (i) *arrowhead formation*, and (ii) *circular formation*. In the two formations, Boid 1, situated initially at $(x_1, y_1) = (8, 24)$ (see Fig. 4(b)and Fig. 6(b)), acts as the leader-boid. As the leader moves towards its target, the follower-boids will move towards the moving ghost target designated to each. These ghost targets of the follower-boids are positioned relative to the position of the leader in a specific pattern (the scheme is illustrated in Fig.2) that will help to maintain the prescribed formation enroute.

5.1. Scenario 1: Arrowhead Formation

For this scenario, the prescribed formation is an arrowhead with the leader boid positioned at the tip of the arrowhead. Assuming the units have been appropriately taken care of, initial conditions pertaining the kinodynamic system and other essentials of the simulation are provided in Table 1.

As the leader moves towards its target, the follower-boids move towards their ghost targets positioned relative to the leader's position, according to the coordinates (a_i, b_i) given in Table 1. From the initial configuration the boids quickly coalesce into a distinct arrowhead formation (Fig. 4(b)). The boids then split from their formation to avoid two obstacles in their path (as shown in Figures 4(c) and 4(d)). After the avoidance, the boids rejoin the flock showing the same prescribed arrowhead formation (Fig. 4(e)). The reformation takes place before the flock reaches the final configuration (Fig. 4(f))

Figure 5(a) shows the evolution of the orientations of the first and the fourth boids. The different headings can be noticed during the split of the flock, however, the pre-defined final orientations are achieved at the target configuration as warranted in this research. Figure 5(b) shows the acceleration components for the leader-boid. One can clearly notice the convergence of the variables at the final state implying the effectiveness of the controllers. Similar trends were observed in the case of the follower-boids. The profiles of the Lyapunov function along the system trajectory show that the conditions of Theorem 1 have been satisfied and that the initial conditions adopted are within the defined domain of the state-space.

Table 1: Numerical values of initial states, constraints and parameters of Scenario 1.

	Initial Conditions
Rectangular positions	$(x_1, y_1) = (8, 24)$, $(x_2, y_2) = (8, 27)$, $(x_3, y_3) = (8, 21)$; $(x_4, y_4) = (8, 30)$, $(x_5, y_5) = (2, 24)$, $(x_6, y_6) = (8, 18)$; $(x_7, y_7) = (2, 30)$, $(x_8, y_8) = (2, 27)$, $(x_9, y_9) = (2, 21)$; $(x_{10}, y_{10}) = (2, 18)$
Angular positions & velo.	$\theta_i = 0$, $\upsilon_i = 0.5$, $\omega_i = 0.8$, for $i = 1$ to 10
	Constraints and Parameters
Dimension of Boids	$l_1 = 1.6$, $l_2 = 1.4$
Target for leader	$(t_{11}, t_{12}) = (50, 24)$, $rt_1 = 0.5$
Final orientations	$t_{i3} = 0$, for $i = 1$ to 10
Position of ghost targets relative to leader boid	$(a_2, b_2) = (3, -3)$, $(a_3, b_3) = (3, 3)$, $(a_4, b_4) = (6, -6)$; $(a_5, b_5) = (6, 0)$, $(a_6, b_6) = (6, 6)$, $(a_7, b_7) = (9, -9)$; $(a_8, b_8) = (9, -3)$, $(a_9, b_9) = (9, 3)$, $(a_{10}, b_{10}) = (9, 9)$;
Fixed obstacles (o_{k1}, o_{k2})	$(o_{11}, o_{12}) = (25, 28)$, $(o_{21}, o_{22}) = (25, 20)$, $ro_1 = ro_2 = 1.5$
Max. translational speed	$\upsilon_{max} = 3$
Min. turning radius	$\rho_{min} = 0.14$
Clearance parameter	$\epsilon_1 = 0.1$, $\epsilon_2 = 0.05$
	Control and Convergence Parameters
Obstacle avoidance	$\alpha_{ik} = 0.6$, for $i = 1$ to 10 and $k = 1$ to 2
Boid avoidance	$\beta_{ij} = 0.01$, for $i = 1$ to 10, $j = 1$ to 10, $i \neq j$
Dynamics constraints	$\gamma_{is} = 0.0001$, for $i = 1$ to 10, $s = 1$ to 2
Convergence	$\delta_{11} = 3$, $\delta_{12} = 3$, $\delta_{iq} = 2$, for $i = 2$ to 10 and $q = 1$ to 2

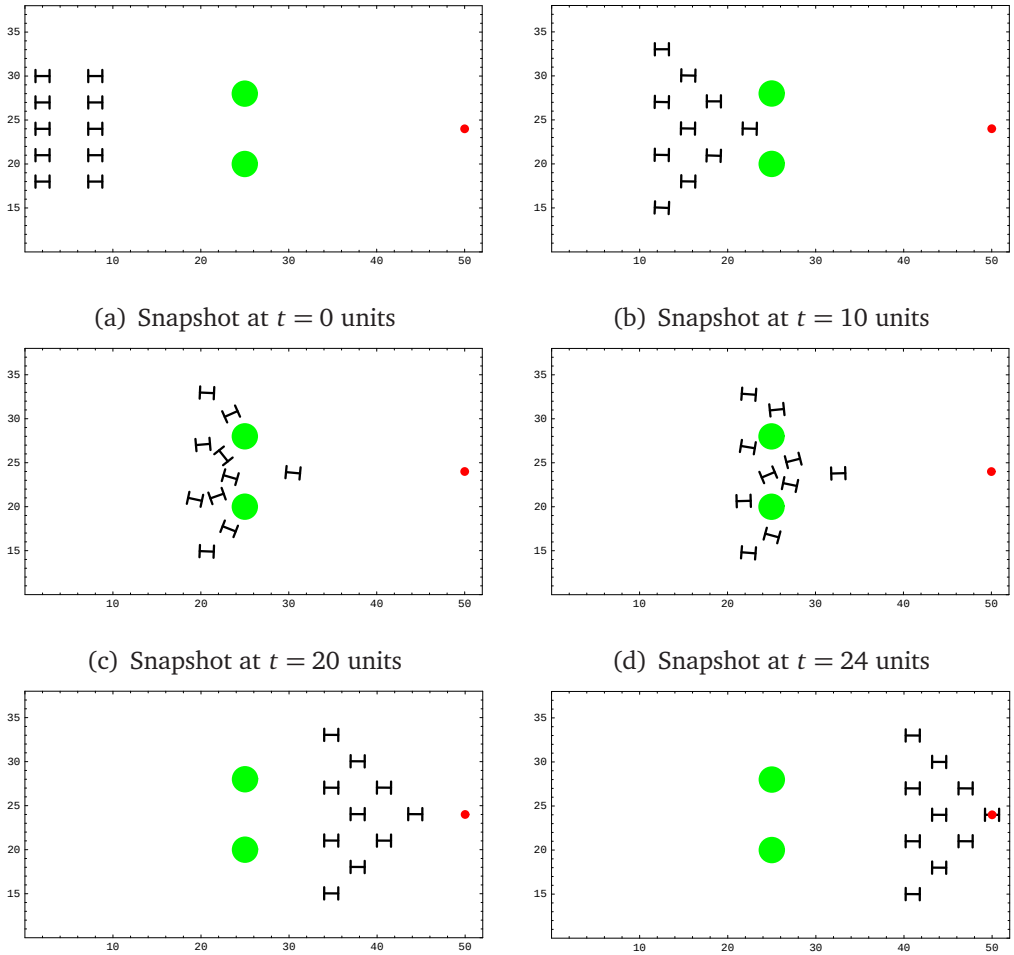

(a) Snapshot at $t = 0$ units

(b) Snapshot at $t = 10$ units

(c) Snapshot at $t = 20$ units

(d) Snapshot at $t = 24$ units

(e) Snapshot at $t = 50$ units

(f) Snapshot at $t = 200$ units

Figure 4: Showing the split/rejoin maneuvers for a flock of 10 nonholonomic boids locked in an arrowhead formation.

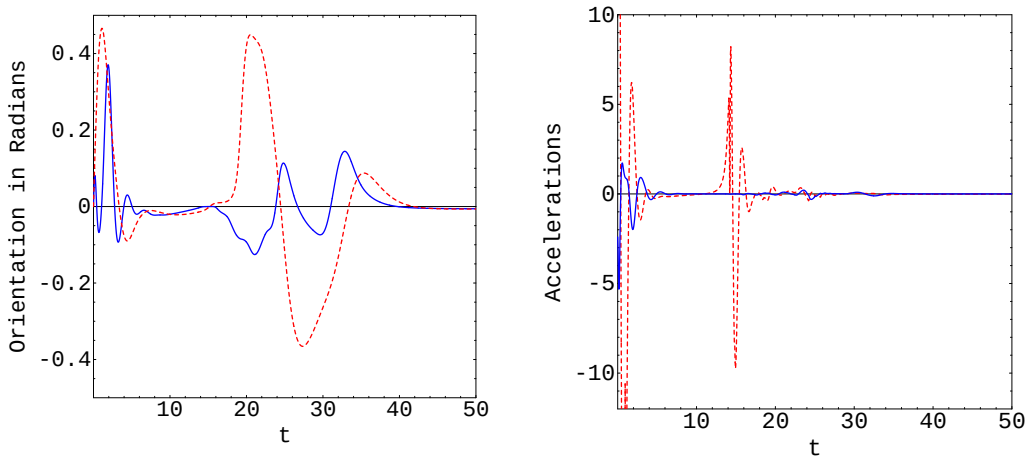

(a) Angular position θ of Boid 1 (dashed line) and Boid 4.

(b) Accelerations: σ (dashed line) and η.

Figure 5: Evolution of the angular positions and acceleration components for Scenario 1.

5.2. Scenario 2: Circular Formation

For this scenario, the prescribed formation is a circular arrangement with the leader-boid positioned in the center of the formation. We retain the leader-follower scheme although the virtual structures/centers could have been utilized for this particular formation. Table 5.2 provides the essentials for the simulation; however, only those that are different from scenario 1.

Figure 6 illustrate a similar split/rejoin maneuver as in scenario 1; however, with a different constellation. The flock establishes the specified formation, carries out the split/rejoin maneuver to avoid the obstacles, re-establishes the formation and finally converges to the final configuration. Figure 7 shows the velocity and acceleration components of Boid 4. Again the figures illustrate the convergent nature of the nonlinear controllers. Similar trends were observed in the case of the other boids.

Table 2: Numerical values of constraints and parameters of Scenario 2.

Position of ghost targets relative to leader boid	$(a_2, b_2) = \kappa(\cos(\frac{\pi}{9}), \sin(\frac{\pi}{9}))$, $(a_3, b_3) = \kappa(\cos(\frac{17\pi}{9}), \sin(\frac{17\pi}{9}))$ $(a_4, b_4) = \kappa(\cos(\frac{\pi}{3}), \sin(\frac{\pi}{3}))$, $(a_5, b_5) = \kappa(\cos(\pi), \sin(\pi))$ $(a_6, b_6) = \kappa(\cos(\frac{5\pi}{3}), \sin(\frac{5\pi}{3}))$, $(a_7, b_7) = \kappa(\cos(\frac{5\pi}{9}), \sin(\frac{5\pi}{9}))$ $(a_8, b_8) = \kappa(\cos(\frac{7\pi}{9}), \sin(\frac{7\pi}{9}))$, $(a_9, b_9) = \kappa(\cos(\frac{11\pi}{9}), \sin(\frac{11\pi}{9}))$ $(a_{10}, b_{10}) = \kappa(\cos(\frac{13\pi}{9}), \sin(\frac{13\pi}{9}))$ where $\kappa = 7$
	Control and Convergence Parameters
Obstacle avoidance	$\alpha_{ik} = 0.6$, for $i = 1$ to 10 and $k = 1$ to 2
Boid avoidance	$\beta_{ij} = 0.01$, for $i = 1$ to 10, $j = 1$ to 10, $i \neq j$
Dynamics constraints	$\gamma_{is} = 0.001$, for $i = 1$ to 10 and $s = 1$ to 2
Convergence	$\delta_{iq} = 3$, for $i = 1$ to 10 and $q = 1$ to 2

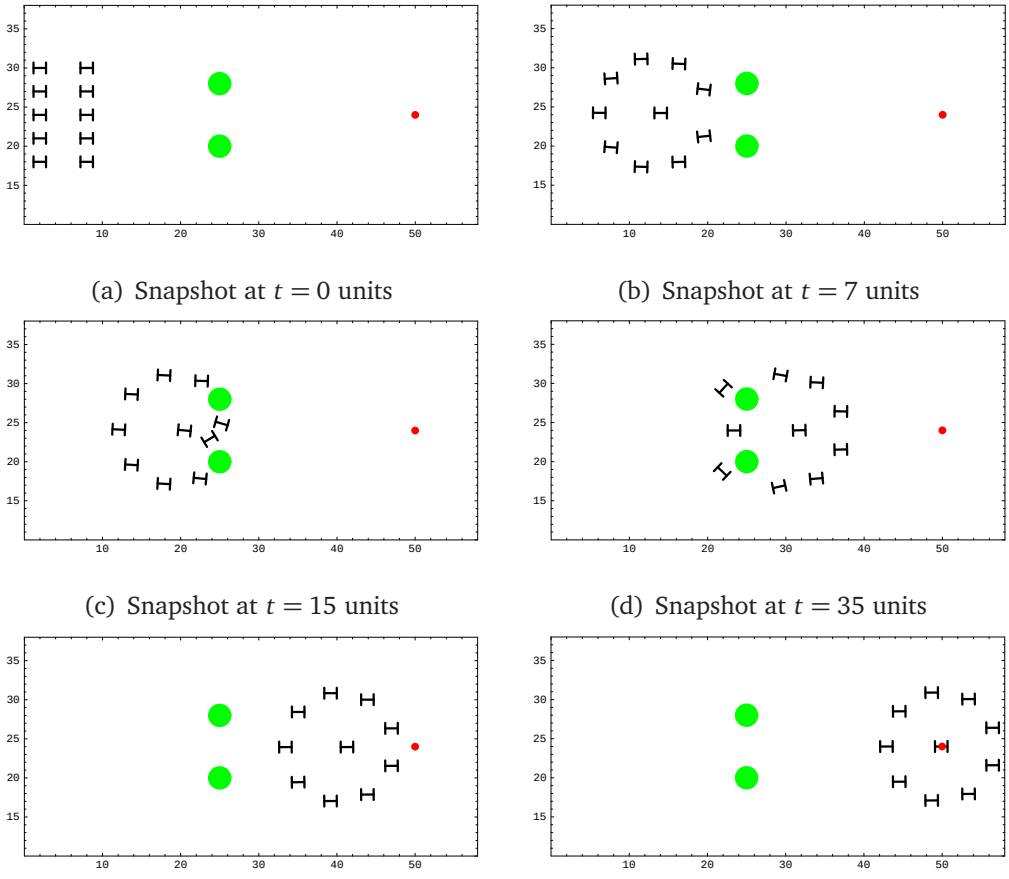

(a) Snapshot at $t = 0$ units

(b) Snapshot at $t = 7$ units

(c) Snapshot at $t = 15$ units

(d) Snapshot at $t = 35$ units

(e) Snapshot at $t = 60$ units

(f) Snapshot at $t = 200$ units

Figure 6: Showing the split/rejoin maneuvers for a group of 10 nonholonomic boids maintained in a circular constellation.

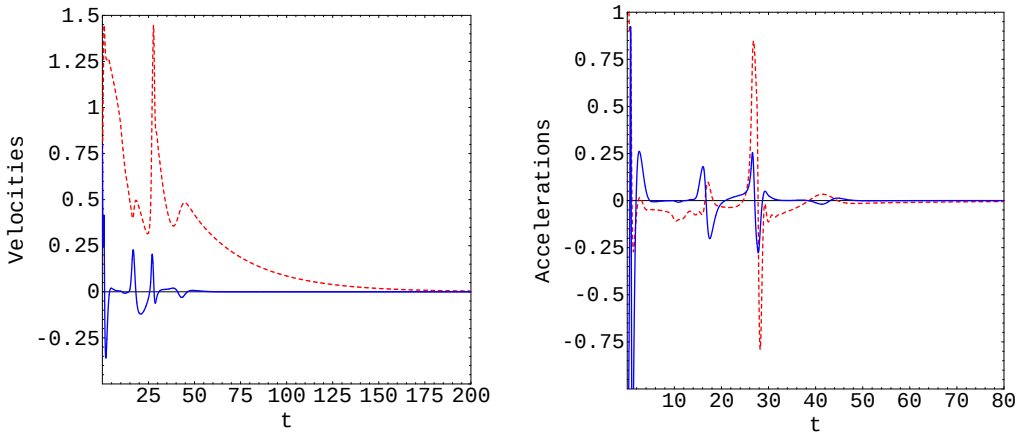

(a) Velocities: v (dashed line) and ω. (b) Accelerations: σ (dashed line) and η.

Figure 7: Evolution of the velocity and acceleration components of Boid 4 for Scenario 2.

6. Conclusion

The Lyapunov-based control scheme was successfully utilized to create a new set of continuous time-invariant control laws. We were able to generate a prescribed formation, accomplish the required split/rejoin maneuvers and re-establish the original formation of a flock of nonholonomic robots. By and large, the control scheme has presented an excellent platform to yield split/rejoin maneuvers of a flock fixed in a arbitrary formation. The new controllers (4.1) and (4.2) produced feasible trajectories and ensured a nice convergence of the system to the equilibrium state, whilst satisfying all the constraints tagged on the system. Moreover, although computationally intensive the control scheme will sufficiently encompass expansions to and scalability of flocks.

The unique pattern of boids' movement as a flock was possible by inclusion of a new leader-follower strategy that involved moving ghost targets which were posi-

tioned relative to the leader-boid. This specific positioning, however, restricted the formation to a horizontal wayward motion only. Future research will address rotation of formations and changing the leadership roles of the flockmates. The authors will also utilize the concept of flocking via the Lyapunov-based control scheme on tunnel passing and lane merging problems of intelligent vehicle systems.

References

[1] C. Belta and V. Kumar. Abstraction and control for groups of robots. In *Reprinted from IEEE Transactions on Robotics and Automation*, volume 4, pages 865–875, October 2004.

[2] R.W. Brockett. *Differential Geometry Control Theory*, chapter Asymptotic Stability and Feedback Stabilisation, pages 181–191. Springer-Verlag, 1983.

[3] D. E. Chang, S. C. Shadden, J. E. Marsden, and R. Olfati-Saber. Collision avoidance for multiple agent systems. In *Procs. of the 42nd IEEE Conference on Decision and Control*, Maui, Hawaii USA, December 2003.

[4] D. Crombie. The examination and exploration of algorithms and complex behavior to realistically control multiple mobile robots. Master's thesis, Australian National University, 1997.

[5] P. Ögren. Formations and obstacle avoidance in mobile robot control. Master's thesis, Royal Institute of Technology, Stockholm, Sweden, June 2003.

[6] L. Edelstein-Keshet. Mathematical models of swarming and social aggregation. In *Procs. 2001 International Symposium on Nonlinear Theory and Its Applications*, pages 1–7, Miyagi, Japan, October-November 2001.

[7] G. H. Elkaim and R. J. Kelbley. A lightweight formation control methodology for a swarm of non-holonomic vehicles. In *IEEE Aerospace Conference*, 2006.

[8] V. Gazi. Swarm aggregations using artificial potentials and sliding mode control. In *Procs. IEEE Conference on Decision and Control*, pages 2041–2046, Maui, Hawaii, December 2003.

[9] W. Kang, N. Xi, J. Tan, and Y. Wang. Formation control of multiple autonomous robots: Theory and experimentation. *Intelligent Automation and Soft Computing*, 10(2):1–17, 2004.

[10] J-C. Latombe. *Robot Motion Planning*. Kluwer Academic Publishers, USA, 1991.

[11] M. Lindhé. A flocking and obstacle avoidance algorithm for mobile robots. Master's thesis, KTH School of Electrical Engineering, Stockholm, Sweden, June 2004.

[12] C. W. Reynolds. Flocks, herds, and schools: A distributed behavioral model, in computer graphics. In *Procs. of the 14th annual conference on Computer graphics and interactive techniques*, pages 25–34, New York, USA, 1987.

[13] B. Sharma. New directions in the applications of the lyapunov-based control scheme to the findpath problem. PhD Dissertation, July 2008.

[14] B. Sharma and J. Vanualailai. Lyapunov stability of a nonholonomic car-like robotic system. *Nonlinear Studies*, 14(2):143–160, 2007.

[15] B. Sharma, J. Vanualailai, and A. Prasad. Formation control of a swarm of mobile manipulators. *Rocky Mountain Journal of Mathematics*, To Appear.

[16] H. Tanner, A. Jadbabaie, and G. J. Pappas. Stable flocking of mobile agents, part i: Fixed topology. In *Procs. of the 42nd IEEE Conference on Decision and Control*, pages 2010–2015, 2003.

[17] R. Olfati-Saber. Flocking for multi-agent dynamic systems: Algorithms and theory. *IEEE Transactions on Automatic Control*, 51(3):401–420, 2006.

[18] R. Olfati-Saber and R. M. Murray. Flocking with obstacle avoidance: Cooperation with limited information in mobile networks. In *Procs. of the 42nd IEEE Conference on Decision and Control*, volume 2, pages 2022–2028, Maui, Hawaii, December 2003.

[19] J. Vanualailai, B. Sharma, and A. Ali. Lyapunov-based kinematic path planning for a 3-link planar robot arm in a structured environment. *Global Journal of Pure and Applied Mathematics*, 3(2):175–190, 2007.